

# Origin and significance of calcium carbonate in soils of southwestern Patagonia

James G. Bockheim \*, Daniel C. Douglass

*University of Wisconsin, at Madison, USA*

Received 31 October 2005; received in revised form 27 April 2006; accepted 11 May 2006

Available online 5 July 2006

## Abstract

A soil chronosequence spanning the last 0.76–1.0 Ma shows a progressive increase in calcium carbonates based on (1) thickness of the Bk+Bck horizons, (2) maximum carbonate stage, (3) profile accumulation of pedogenic carbonates, and (4) mass flux of Ca from a geochemical mass balance. We favor a dust origin of the carbonates because (1) the till parent materials contain low amounts of CaCO<sub>3</sub>, (2) there is minimal evidence for weathering of Ca-bearing minerals in the soil, (3) the amount of CaCO<sub>3</sub> in the profile is far in excess of what could be released by weathering, (4) dust collected from the study area is enriched in CaCO<sub>3</sub>, and (5) a source area for the carbonates was identified. Although there likely were changes in dust deposition rates during the Quaternary, our calculations suggest that the current deposition rate of 0.18 g CaCO<sub>3</sub> m<sup>-2</sup> yr<sup>-1</sup> is comparable to the long-term profile accumulation rate of 0.16 g CaCO<sub>3</sub> m<sup>-2</sup> yr<sup>-1</sup>. <sup>230</sup>Th/U disequilibrium ages of carbonate pendants are consistent with cosmogenic surface-exposure ages indicating that this method has potential for dating other geomorphic surfaces in Patagonia. Cryogenic processes have affected many of the pedons, particularly during the last glacial maximum.

© 2006 Elsevier B.V. All rights reserved.

*Keywords:* Dust; CaCO<sub>3</sub>; Patagonia; Pedogenesis; Soil chronosequence

## 1. Introduction

There is considerable debate regarding the origin of CaCO<sub>3</sub> and petrocalcic horizons (calcretes) in semi-arid soils of Patagonia. Trombotto (1996) points out the paucity of carbonate-rich sediments in Patagonia and argues that the Ca originates lithogenically, i.e., from soil weathering; in contrast, a second group (Vogt and del Valle, 1994; Zárate, 2003) proposed that the carbonates were deposited as dust from an expanded inner coastal shelf during Quaternary cold periods. Although we recognize that carbonate deposition rates have varied during the

Quaternary, we will demonstrate that the carbonates are being deposited today as dust at rates that are consistent with profile quantities of CaCO<sub>3</sub>.

Not only is dust important in pedogenesis, but also a Patagonian source of dust has been identified during glacial stages 2, 4 and 6 in Antarctic ice cores (Basile et al., 1997; Delmonte et al., 2004a,b). Rare-earth elements and Sr–Nd isotopic data have been particularly useful in showing a Patagonian source for the dust (Smith et al., 2003; Delmonte et al., 2004b).

Key hypotheses of this study are:

- (1) carbonates in soils of the Lago Buenos Aires area originate from dust rather than from pedogenic weathering;

\* Corresponding author.

E-mail address: [bockheim@wisc.edu](mailto:bockheim@wisc.edu) (J.G. Bockheim).

- (2) the amount of carbonates in contemporary dust projected over the long-term generally is consistent with profile quantities of  $\text{CaCO}_3$ ;
- (3) pedogenic carbonates are a key relative-age indicator in southern Patagonia; and
- (4) pedogenic carbonates offer promise for dating sediments in Patagonia.

## 2. Study area

The study was conducted along a 40-km transect from just west of the city of Perito Moreno to the Arroyo Telken lava flow (Fig. 1). Based on a decade of weather observations and longer regional records, the mean annual air temperature is  $9\text{ }^\circ\text{C}$  and the mean annual precipitation is  $200\text{ mm yr}^{-1}$  (National Center for Atmospheric Research, 2003). Average summer (Dec.–Feb.) and winter (June–Aug.) temperatures are  $14\text{ }^\circ\text{C}$  and  $3\text{ }^\circ\text{C}$ , respectively. Approximately 75% of the annual precipitation falls from late fall through early spring (April to September). Summer winds are strong and persistently from the west; winter winds are weaker and more variable.

We collected data over a 20-month period using onset data loggers at two sites with the following results (1) the

mean annual air temperature from January 2004 to January 2005 was  $8.0\text{ }^\circ\text{C}$ , (2) the mean annual soil temperature at 50 cm was  $10\text{ }^\circ\text{C}$ , (3) the soil moisture content at 25 cm averaged  $0.10\text{ m}^3\text{m}^{-3}$ , and (4) the soil moisture regime appears to be xeric at elevations from ca. 500–700 m and aridic at elevations below 500 m (Fig. 2).

The study area is part of the Southern Patagonian Steppe eco-region and contains shrub–steppe and grass–steppe vegetation types (Soriano, 1983); the amount of bare ground varies from 40–70%. Dominant plant species include coirón bunchgrass (*Stipa humilis*) and neneo (*Mulinum spinosum*), with occasional calafate (*Berberis heterophylla*) and molle (*Schinus johnstonii*) shrubs.

The Quaternary geomorphology of southern Argentina is comprised of spectacular sequences of glacial moraines and associated outwash terraces (Clapperton, 1993). During ice ages, mountain glaciers expanded and coalesced to form the Patagonian Ice Cap. Outlet glaciers eroded deep valleys through the mountains and advanced out onto the flat plains east of the Andes at some locations. In the Lago Buenos Aires valley, glaciers advanced as far as 100 km from the mountain front. Dating of the glacial landforms is based on three

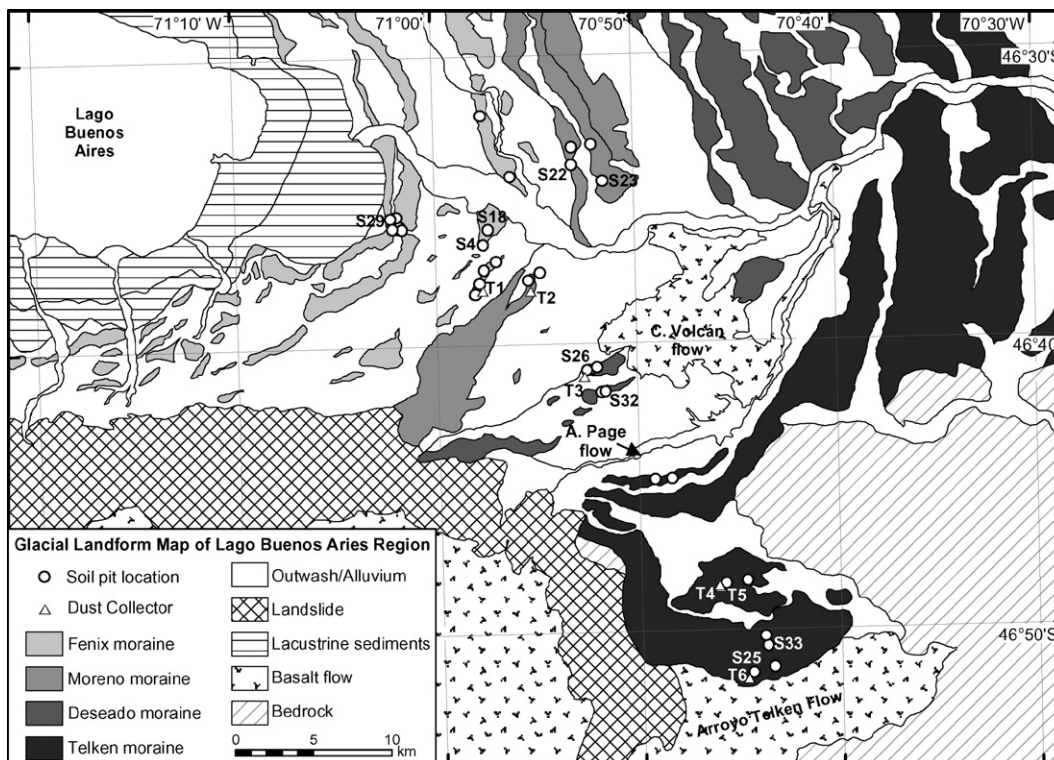


Fig. 1. Location of study area in the Lago Buenos Aires area.

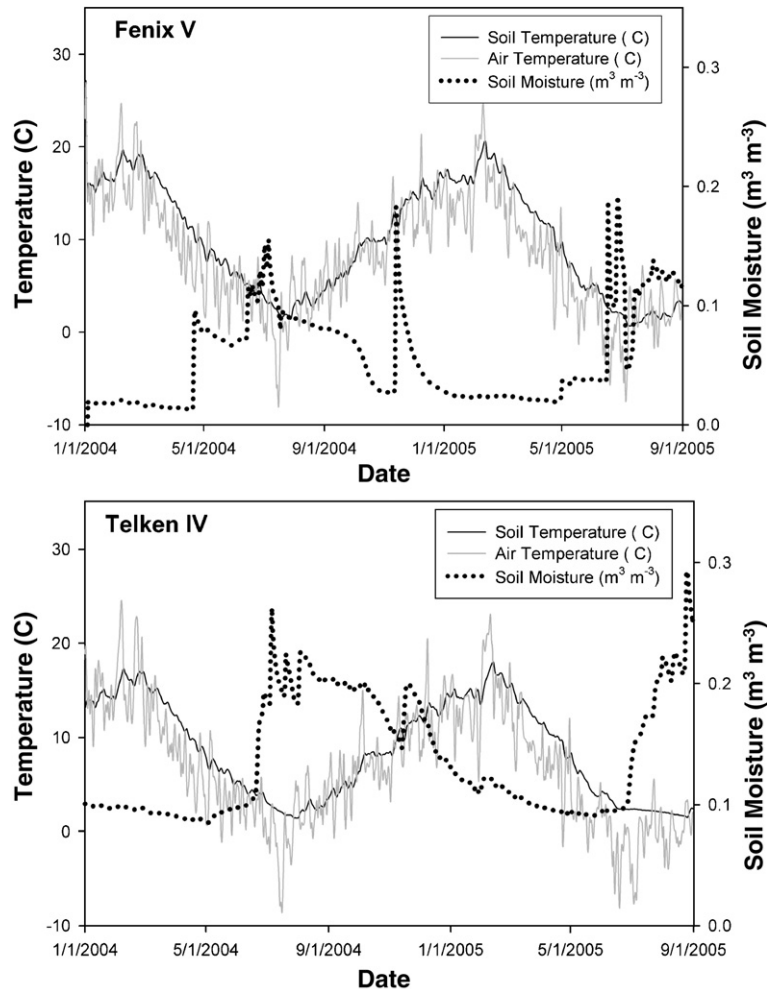


Fig. 2. Weather data for the period January 1, 2003–Dec. 31, 2004, including air temperature, soil temperature at 50 cm, and soil moisture at 25 cm on (A) Fenix V (S46° 37′52.8″, W070°57′46.5″) and (B) Telken IV (S46°45′25.6″, W070°45′48.2″) moraines.

young basalt flows and about 100 cosmogenic-nuclide surface-exposure ages. Based on these ages, the chronology includes the Menucos drift (14.4 ka), Fenix I–V drifts (15.8–22.7 ka), Moreno I–III drifts (~150 ka), Deseado I–III drift (~350–760 ka), and Telken I–VI drifts (760–1016 ka) (Singer et al., 2004; Kaplan et al., 2004).

A 1:2 million-scale soil map of Santa Cruz province shows Xerorthents on Menucos and Fenix surfaces and Haplargids on older surfaces (INTA, 1995). However, our data show that all of the soils contain a mollic epipedon; therefore, we classify the soils as Haploxerolls and Calcixerolls, respectively (Douglass and Bockheim, 2006). Moreover, the clay enrichment in the Bk horizon of Telken soils does not reflect argilluviation. Douglass and Bockheim (2006) provided descriptions of the soils considered in this study.

### 3. Methods

#### 3.1. Field

We sampled 34 pedons on or near moraine crests in locations that appeared to be stable and have representative vegetation cover and surface boulder frequency. Soils were excavated by hand and described according to Schoeneberger and others (2002). Stages of carbonate morphology were identified using criteria of Gile et al. (1966) as modified by Birkeland (1999). Percentages of coarse fragments were visually estimated in the exposed wall of the soil pit. Bulk samples were passed through a 2-mm sieve in the field. The fine-earth fraction was returned to the laboratory for characterization.

Bulk density was measured for 9 of the 34 soil profiles using the compliant cavity procedure (method 4A5, Soil

Survey Staff, 1996) and corrections were applied for the >2 mm coarse-fragment content. Data from these profiles were used to generate an equation that was used to estimate bulk density for other soil horizons (Douglass and Bockheim, 2006). Three minimally disturbed, oriented samples were collected from the A2 and Bk horizons of Deseado II and Telken IV pedons in galvanized sheet-metal “Kubiena containers” measuring 6.0 cm × 20 cm × 5.0 cm deep for preparation of thin sections.

Stage I carbonate rinds (coatings) on coarse-gravel (7.5 cm diameter) clasts collected from Fenix, Moreno, and Deseado drifts were dated using the  $^{230}\text{Th}/\text{U}$  method and thermal ionization mass spectrometry at the Berkeley Geochronology Center (Sharp et al., 2003).

Six dust collectors were installed along a transect from LBA to Estancia Telken in January 2003 (locations shown in Fig. 1) to measure dust composition and deposition rates. We used plastic dishpans measuring 35 by 30 cm and 11 cm deep that contained a 2.5-cm depth of marbles. The dust traps were positioned 50–75 cm above the ground surface on rock cairns to reduce sampling the local saltating load. Samples were collected in January 2004

and October 2005. During the first year, we obtained a reliable sample for dust deposition rates from only one collector; five of six collectors yielded samples during the second sampling interval. We were unable to collect dust samples where wind or sheep had disturbed the collectors or where humans had removed them.

### 3.2. Laboratory

Soil samples were sent to the University of Missouri Soil Characterization Laboratory, where analyses were performed using methods established by the Soil Survey Staff (1996), including particle-size distribution with sand fractionation (method 3A), pH and electrical conductivity in distilled water (8Cl<sub>a</sub> and 8I, respectively),  $\text{NH}_4\text{OAc}$ -extractable bases (5B1),  $\text{BaCl}_2$ -triethanolamine-extractable acidity (6H1), cation-exchange capacity (CEC) by  $\text{NH}_4\text{OAc}$  at pH 8.2 (5A2), and base saturation from summation. Total organic and inorganic carbon were measured with a Leco CNS-2000 analyzer. Samples from each horizon were homogenized and pulverized to pass a 100-mesh sieve. Two samples were analyzed for each

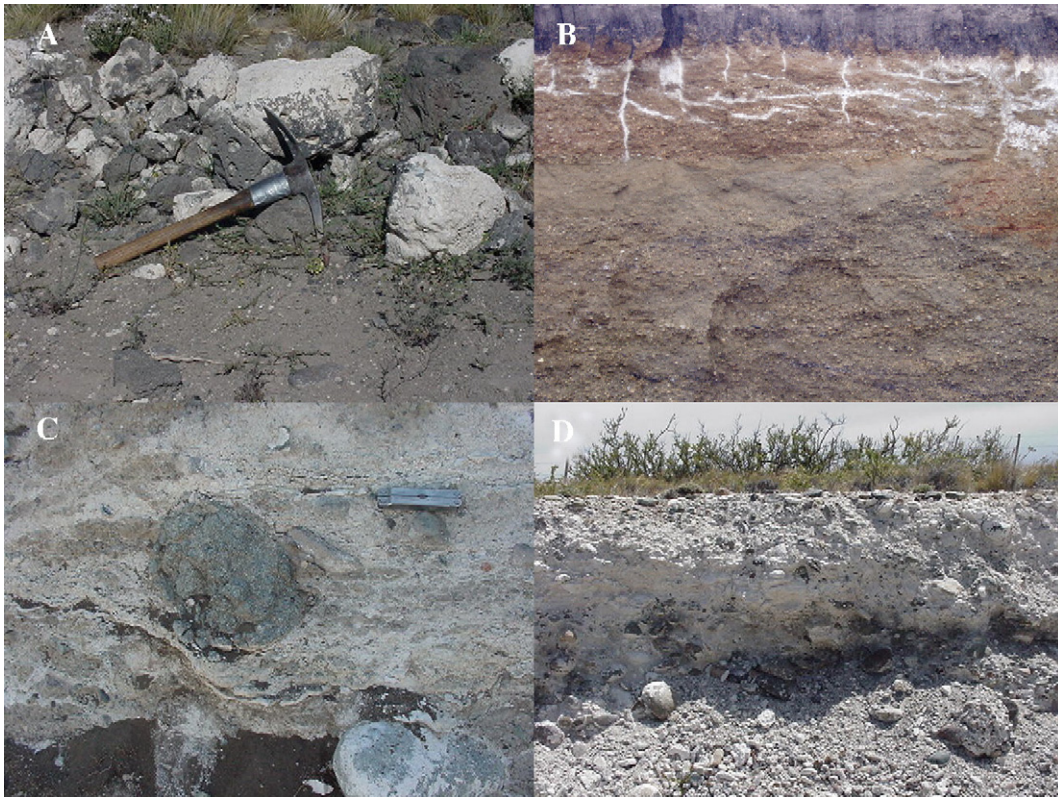


Fig. 3. Morphological features of carbonates in soils from the LBA area, including (A) stage I carbonate encrustations in a Menucos soil; (B) carbonate seams in alluvial fan materials of mid-Pleistocene age near Río Gallegos; (C) stage IV carbonates in Telken IV soil; and (D) stage V carbonates in soil in a Telken V soil.

horizon; an untreated sample was used to determine the total carbon content of the soil (i.e., organic carbon plus carbonate). The other sample was heated at 300 °C in a muffle furnace for 24 h to combust organic material and was then used to determine the carbonate content of the soil. Organic carbon was calculated as the difference between total carbon and carbonate content. Combustion temperatures inside the LECO are ~1300 °C, high enough to oxidize all forms of carbonate. We were unable

to differentiate between calcite and other forms of carbonate, such as dolomite.

The following measurements were performed on dust samples: (1) organic C and CaCO<sub>3</sub> using the methods described for soils and (2) total elemental analysis as described in the following section.

Nine of the thirty-four pedons described in Douglass and Bockheim (2006) were selected for detailed chemical analysis. These pedons displayed representative soil

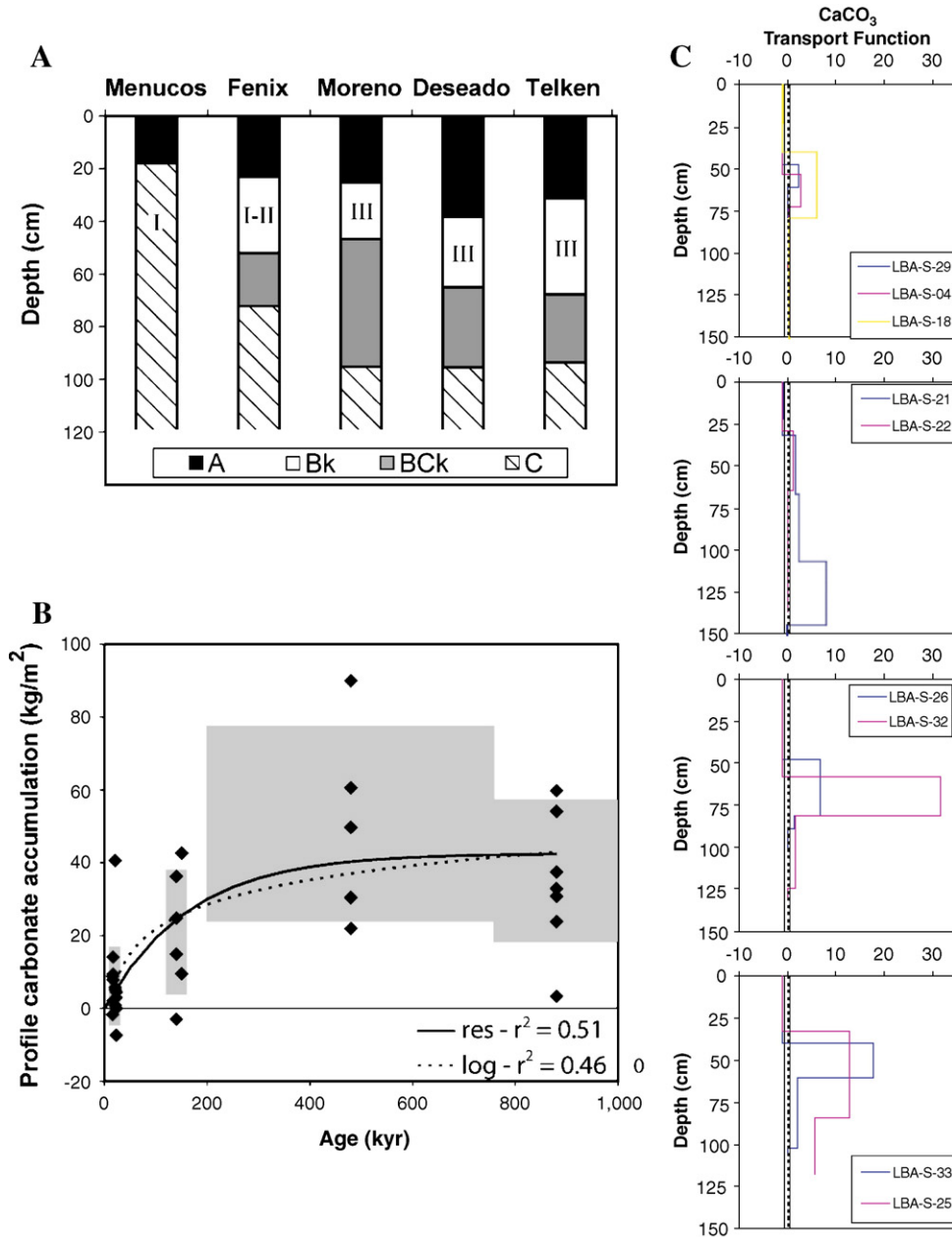


Fig. 4. Relation between time of exposure and (A) thickness of the Bk+Bck horizon and carbonate morphology stage; (B) profile quantities of carbonates; and (C) transport function of carbonates from a geochemical mass balance.

morphology for their moraine groups and were sampled to un-weathered parent material in most cases. Elemental composition was measured on the fine-earth (<2 mm) fraction, the silt+clay fraction (<50  $\mu\text{m}$ ), and the medium+fine sand fraction (0.50–0.10 mm). The latter two fractions typically represent  $\sim 65\%$  of the fine-earth fraction. Samples were ground in a micro ball mill and sent to Activation Laboratories Ltd. (Ancaster, Ontario) for measurement of major-oxide and trace-element concentrations by inductively coupled plasma emission spectrometry following fusion with lithium metaborate/tetraborate. Elements analyzed include Si, Al, Fe, Mn, Mg, Ca, Na, K, Ti, P, Ba, Sr, Y, Sc, Zr, Be, and V, as well as loss on ignition.

Thin sections were prepared using the techniques of FitzPatrick (1993). Samples were impregnated with epoxy resin under a vacuum and cured for a minimum of 24 h; oriented sections were cut with a diamond saw and cemented onto glass microscope slides. The slides were ground and polished to a thickness of 30  $\mu\text{m}$  and examined under natural and polarized light with a polarizing microscope.

### 3.3. Calculations and statistics

Profile quantities of  $\text{CaCO}_3$  were determined by multiplying the percent by mass of the constituent by the bulk density and the thickness of the horizon, with a correction for the percentage of coarse fragments in the soil; horizon values were summed to determine the profile quantity (Bockheim et al., 2000). The percent by mass of the constituent in the parent material was subtracted from the horizon value to account for the original starting composition. Profile quantities of carbonates were regressed against time of exposure using two mathematical models, a logarithmic model ( $y=A+\ln B$ ) and a reservoir model that consists of a linear input function and a loss function that is dependent on the concentration of the constituent (i.e. a zero-order input function and first-order loss) (Douglass and Bockheim, 2006).

We calculated long-term accumulation rates (LTA) of carbonates as the total amount of carbonate accumulation divided by the age of the soil (Schlesinger, 1990; Bockheim et al., 2000). This analysis assumes that the accumulation rate of the constituent in the soil is constant.

Geochemical mass balances were used to calculate the gain and loss of elements, as well as the translocation of elements within selected pedons (Brimhall and Dietrich, 1987). The method is based on the principle of conservation of mass and the ability to determine the volumetric change of the soil during the weathering process. Uncertainties of the method for soils in the LBA

area are described in detail in Douglass and Bockheim (2006).

The statistical significance of trends in the data was tested using analysis of variance (ANOVA) and Fisher's test of least probabilities using a MINITAB software package (MINITAB, Inc., 2000).

## 4. Results

There was a progressive increase in carbonate stage with time of exposure, including from youngest to oldest: Menucos, stage I; Fenix stage I–II; Moreno and Deseado stage III; and Telken, stage III+–IV (Figs. 3 and 4A). Similarly, the thickness of the Bk+BCk horizons increased with soil age (Fig. 4A); however, the differences were not statistically significant. Profile accumulation of carbonates increased sharply with age in Fenix to Deseado soils but appeared to equilibrate in Telken soils, particularly in the case of the reservoir model (Fig. 4B). Transport functions calculated from geochemical mass balance

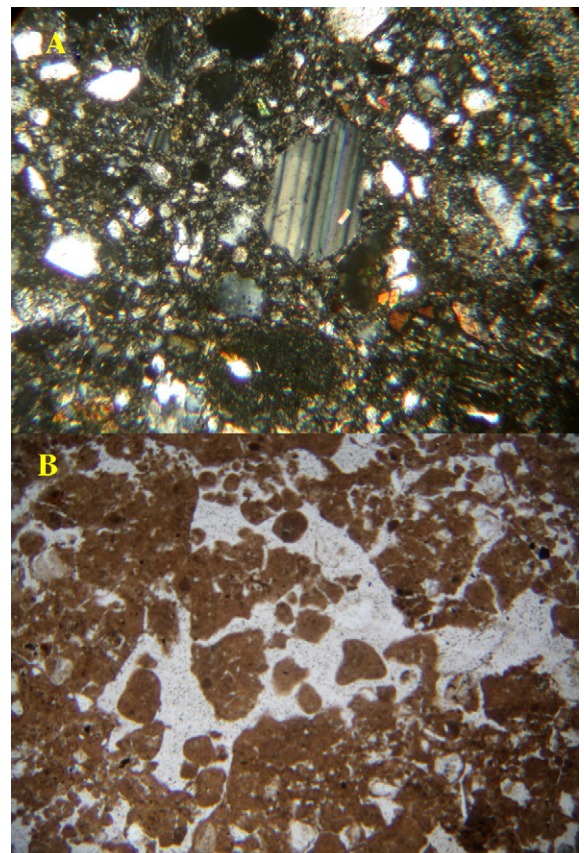


Fig. 5. Thin sections showing (A) minimal weathering of plagioclase grains in the Bk2 horizon of a soil on Deseado drift (cross polar; 0.6 mm across) and (B) carbonate nodules (encased in white) in the Bk horizon of a soil on Telken drift (plain light, 2.4 mm across).

Table 1  
Key properties of soils in the Lagos Buenos Aires area, southern Patagonia

Horizon	Depth cm	Grain size distribution (%)										pH	EC dS/m	OC %	CaCO <sub>3</sub> %	Exchangable ions (cmol (+) kg <sup>-1</sup> )								Base Sat. %
		Total			Silt fraction		Sand fractions									Ca	Mg	Na	K	Sum	Neut.	Sum	Sum	
		Clay	Silt	Sand	F	C	VF	F	M	C	VC					Bases	Acid.	Cations	CEC					
Fenix I Moraine (~ 16 ka)																								
LBA-S-29																								
A	0–23	3	11	86	5	6	14	26	14	17	16	6.66	0.30	0.7	0.0	5.1	1.2	0.1	0.5	6.8	1.9	8.7	9.0	78
Bw	23–48	4	24	72	12	13	17	23	10	11	10	7.05	0.30	0.4	0.0	7.4	1.6	0.2	0.1	9.3	1.3	10.6	9.8	87
Bk	48–61	4	18	78	9	8	13	24	13	15	14	7.98	0.36	0.3	5.3	31.6	1.6	0.4	0.1	33.6	0.0	33.6	6.6	100
2C	61–79	3	47	50	30	18	17	18	6	5	5	7.99	0.37	0.4	6.1	31.0	2.0	0.4	0.1	33.5	0.0	33.5	7.8	100
Fenix IV Moraine (~ 22 ka)																								
LBA-S-04																								
A	0–18	11	35	54	16	19	16	15	7	2	15	6.94	0.31	0.9	0.0	6.8	1.9	0.1	0.9	9.7	2.5	12.2	11.1	80
Bw	18–53	9	31	60	19	13	15	14	7	11	12	7.02	0.28	0.6	0.0	6.3	1.6	0.1	0.6	8.6	2.8	11.4	10.1	75
Bk	53–72	6	37	57	22	15	17	15	7	9	9	8.15	0.33	0.2	3.6	25.2	2.0	0.2	0.3	27.8	0.0	27.8	7.6	100
BCk	72–105	4	32	64	17	15	19	15	7	12	13	8.65	0.47	0.1	1.5	12.8	2.4	1.0	0.3	16.5	0.0	16.5	6.0	100
C	105–110	5	34	62	19	15	15	15	8	13	12	8.58	0.70	0.1	1.1	11.9	2.4	1.7	0.4	16.4	0.0	16.4	5.8	100
LBA-S-18																								
A	0–23	4	10	87	4	6	18	26	16	16	10	6.45	0.25	0.5	0.0	4.0	1.2	0.1	0.7	6.0	2.0	8.0	6.8	75
Bw	23–40	7	17	76	9	8	14	28	15	13	8	7.06	0.29	0.4	0.0	6.5	2.0	0.1	0.4	9.1	3.5	12.6	9.5	72
Bk	40–79	9	39	52	28	12	9	10	6	11	14	8.31	0.36	0.3	12.4	35.9	3.2	0.2	0.1	39.4	0.0	39.4	7.3	100
BCk	79–155	3	47	51	25	22	15	11	6	9	10	8.35	0.31	0.1	2.1	18.8	1.6	0.2	0.1	20.7	0.0	20.7	4.8	100
Moreno I Moraine (~ 140 ka)																								
LBA-S-22																								
A1	0–19	2	6	91	3	3	20	34	14	12	11	7.20	0.34	0.7	0.0	5.3	0.8	0.0	0.8	6.9	0.6	7.5	7.9	92
A2	19–29	11	23	67	14	9	15	21	9	10	11	7.02	0.34	1.1	0.0	9.5	1.6	0.1	0.7	11.9	2.6	14.4	13.0	82
Bk	29–65	4	23	73	13	10	11	17	10	16	19	8.24	0.34	0.1	2.3	27.1	1.2	0.2	0.1	28.6	0.0	28.6	5.8	100
BCk	65–137	2	20	79	10	10	12	20	12	15	21	8.36	0.33	0.1	1.4	16.7	1.6	0.2	0.1	18.5	0.0	18.5	4.9	100
Moreno II Moraine (~ 150 ka)																								
LBA-S-23																								
A	0–22	2	7	91	4	4	28	31	10	10	13	6.84	0.31	0.7	0.0	6.0	1.2	0.1	0.4	7.7	0.9	8.6	7.8	89
Bw	22–32	9	24	67	13	11	12	13	8	14	21	6.83	0.30	0.6	0.0	28.8	1.6	0.2	0.0	30.6	0.0	30.6	6.2	100
Bk	32–67	1	30	69	13	17	17	20	9	11	12	8.01	0.38	0.1	2.1	19.3	1.2	0.2	0.0	20.7	0.0	20.7	5.3	100
BCk1	67–107	6	28	66	16	12	10	13	7	14	22	8.11	0.40	0.1	4.0	29.6	1.9	0.2	0.0	31.8	0.0	31.8	6.7	100
BCk2	107–145	5	42	53	29	13	6	6	4	11	27	8.45	0.33	0.1	8.7	36.9	6.3	0.7	0.0	43.9	0.0	43.9	9.2	100

(continued on next page)

Table 1 (continued)

Horizon	Depth cm	Grain size distribution (%)										pH	EC dS/m	OC %	CaCO <sub>3</sub> %	Exchangable ions (cmol (+) kg <sup>-1</sup> )								Base Sat. Sum %
		Total			Silt fraction		Sand fractions									Ca	Mg	Na	K	Sum	Neut.	Sum	CEC	
		Clay	Silt	Sand	F	C	VF	F	M	C	VC													
Deseado I Moraine (200–760 ka)																								
LBA-S-26																								
A1	0–36	6	9	85	4	5	18	33	14	11	9	6.95	0.34	0.6	0.0	7.9	1.6	0.1	0.3	10.0	1.4	11.4	10.9	87
A2	36–48	6	10	83	6	4	9	27	21	16	10	7.24	0.35	0.3	0.0	8.7	1.9	0.1	0.2	11.0	1.3	12.2	11.0	90
Bk1	48–81	7	18	75	12	7	9	25	20	13	9	7.95	0.43	0.2	7.7	37.9	3.1	0.2	0.1	41.3	0.0	41.3	9.6	100
Bk2	81–89	9	36	55	23	13	11	12	6	11	15	8.16	0.43	0.2	4.8	34.2	4.3	0.3	0.1	38.9	0.0	38.9	13.5	100
2C	89–100	5	38	57	22	17	18	16	8	8	7	8.33	0.32	0.2	0.0	13.7	4.7	0.3	0.2	18.9	0.0	18.9	15.4	100
Deseado II Moraine (200–760 ka)																								
LBA-S-32																								
A	1–14	6	7	87	4	4	11	27	18	16	15	6.62	0.34	0.7	0.0	6.3	1.5	0.1	0.8	8.6	1.1	9.7	8.8	89
AB	14–58	13	13	74	10	3	3	7	10	27	27	6.96	0.39	0.5	0.0	12.5	2.4	0.2	0.2	15.2	2.6	17.8	15.9	86
Bk	58–81	10	18	72	12	6	7	10	9	22	24	7.87	0.44	0.5	18.4	43.3	4.4	0.3	0.1	48.2	0.0	48.2	10.5	100
BCk	81–125	5	11	84	8	3	3	7	9	29	36	8.10	0.34	0.2	1.9	17.2	3.2	0.2	0.1	20.7	0.0	20.7	7.4	100
C	125–130	9	9	82	7	2	3	8	12	28	31	8.03	0.33	0.0	0.8	11.7	3.7	0.2	0.2	15.8	0.7	16.4	9.3	96
Telken V Moraine (760–1016 ka)																								
LBA-S-33																								
A	0–40	11	14	75	8	6	15	21	12	14	14	7.22	0.47	1.1	0.0	24.1	2.3	0.1	0.6	27.2	1.1	28.3	16.1	96
Bk	40–60	19	33	48	26	7	5	12	10	11	9	7.96	0.47	0.6	26.9	42.7	4.0	0.2	0.3	47.1	0.0	47.1	13.2	100
BCk	60–102	16	38	46	17	21	14	18	8	0	6	8.58	0.40	0.1	5.1	41.6	8.5	0.5	0.3	51.0	0.0	51.0	15.9	100
C	102–105	14	31	55	19	13	13	16	7	9	11	8.55	0.48	0.1	2.0	26.1	6.0	0.6	0.3	33.0	0.0	33.0	11.6	100
Telken VI Moraine (760–1016 ka)																								
LBA-S-25																								
A1	0–20	26	13	61	7	6	14	21	10	8	9	6.79	0.57	1.7	0.0	21.2	5.2	0.1	1.1	27.6	4.3	31.9	29.6	86
A2	20–33	39	16	46	10	5	7	9	8	11	12	7.07	0.56	1.4	0.0	33.4	9.5	0.2	0.7	43.9	7.4	51.2	46.1	86
Bk	33–84	17	29	55	21	8	11	11	7	13	14	8.10	0.47	0.3	12.0	51.8	11.1	0.4	0.4	63.8	1.1	64.9	34.0	98
BC	84–118	6	20	74	12	8	11	13	9	18	24	8.10	0.42	0.1	6.3	45.8	12.3	0.6	0.3	58.9	0.7	59.6	30.4	99

Physical and chemical properties of representative soils from the Lago Buenos Aires area, southern Patagonia.



Table 2  
Deposition rate and composition of dust from the Lagos Buenos Aires area

Location	Deposition rate		Organic C	Carbonate
	(g m <sup>-2</sup> yr <sup>-1</sup> )		(%)	(%)
	2004	2005	2004	2004
Fenix Va	–	3.3	–	–
Fenix Vb	–	21.4	–	–
Moreno	–	–	3.7	4.9
Deseado	–	–	1.6	1.4
Telken IVa	27.1	7.4	3.4	4.4
Telken IVb	–	4.2	–	–
Telken VI	–	3.5	5.9	5.4
Average	27.1	8.0	3.7	4.0

Amount and composition of dust samples from the LBA area.

illustrate the progressive accumulation of CaCO<sub>3</sub> in Bk and Bck horizons (Fig. 4C).

There appears to be minimal chemical weathering of soils in southern Patagonia. Thin sections show fresh plagioclase feldspar grains (Fig. 5A). Geochemical mass-balance shows minimal weathering of aluminosilicate

minerals (Douglass, 2005) but substantial input of CaCO<sub>3</sub> (Fig. 4C). Microfabric analysis verifies field evidence that the carbonates are pedogenic, including the presence of CaCO<sub>3</sub> nodules (Fig. 5B). Older surfaces showed classical forms of stage III +and IV carbonates (Gile et al., 1966; Rabenhorst and Wilding, 1986; Monger et al., 1991), including a whitish cast for >90% of the horizon (Fig. 3D), cappings on columns and prisms, a weak platy structure, laminations (Fig. 3C), and >20% CaCO<sub>3</sub> content (Table 1).

Three different layers of carbonate rinds from a clast from Deseado outwash yielded <sup>239</sup>U–<sup>230</sup>Th ages of 224, 209, and 24 ka (Sharp, personal communication).

## 5. Discussion

Our data support a dust origin of carbonates in soils of the LBA area. The parent materials generally contain low amounts of CaCO<sub>3</sub> (Table 1). There is minimal evidence for weathering of Ca-bearing minerals in soils, based on examination of thin sections (Fig. 5A) and geochemical mass-balance (Fig. 4C). Dust is enriched (~4%) in

Table 3  
Total elemental analysis of dust and the surface A horizon of soils in the Lagos Buenos Aires area

Dust	SiO <sub>2</sub>	Al <sub>2</sub> O <sub>3</sub>	Fe <sub>2</sub> O <sub>3</sub>	MnO	MgO	CaO	Na <sub>2</sub> O	K <sub>2</sub> O	TiO <sub>2</sub>	P <sub>2</sub> O <sub>5</sub>	LOI	TOTAL	Ba	Sr	Y	Sc	Zr	Be	V
	%													ppm					
Moreno	58.52	13.6	5.3	0.12	1.51	3.28	3.5	2.16	1.01	0.37	10.79	100.2	558	314	28	13	243	2	80
Deseado	63.3	13.62	5.42	0.12	1.52	3.15	3.34	2.11	1.02	0.27	5.09	99.0	566	314	24	13	227	2	96
Telken 4	56.11	14.21	5.49	0.14	1.54	3.36	3.8	2.01	1.12	0.38	11.14	99.3	585	322	32	14	258	3	74
Telken 6	53.51	13.87	5.53	0.13	1.52	3.33	3.4	1.97	1.07	0.41	15.27	100.0	542	336	28	14	221	3	83
Average	57.86	13.83	5.44	0.13	1.52	3.28	3.51	2.06	1.06	0.36	10.57	99.6	563	322	28	14	237	3	83
SD	4.16	0.28	0.10	0.01	0.01	0.09	0.20	0.09	0.05	0.06	4.18	0.6	17.9	10.4	3.3	0.6	16.7	0.6	9.3
A horizon %													ppm						
LBA-S-29	45.47	10.34	5.3	0.174	1.55	3.29	6.75	1.48	1.097	12.81	10.99	99.3	564	259	31	14	326	2	88
LBA-S-04	54.17	13.03	5.67	0.126	1.45	2.26	4.49	2.17	0.931	6.03	9.28	99.6	522	200	33	16	198	2	97
LBA-S-18	43.14	10.59	5.25	0.143	1.36	2.64	8	1.58	0.881	15.17	10.32	99.1	462	203	30	15	291	2	88
LBA-S-21	41.04	10.72	5.39	0.128	1.45	3.1	7.81	1.41	0.888	15.06	11.87	98.9	452	238	29	16	195	2	91
LBA-S-22	34.2	8.94	4.86	0.116	1.34	3.27	9.14	1.26	0.753	19.23	15.46	98.6	373	203	27	15	113	2	86
LBA-S-26	43.29	12.22	6.11	0.129	1.47	2.7	5.79	1.45	1.012	10.3	14.69	99.2	399	211	28	17	181	2	105
LBA-S-32	47.66	14.05	6.3	0.13	1.62	2.64	4.26	1.8	1.079	5.87	13.41	98.8	471	213	26	18	242	2	107
LBA-S-33	43.04	12.44	6.33	0.124	1.87	4.24	4.8	1.43	0.934	8.67	14.99	98.9	385	222	29	17	108	2	110
LBA-S-25	46.81	13.54	6.58	0.122	1.77	2.61	3.55	1.59	0.999	5.21	16.24	99.0	384	201	28	18	94	2	104
Avg.	44.31	11.76	5.75	0.13	1.54	2.97	6.07	1.57	0.95	10.93	13.03	99.0	446	217	29	16	194	2	97
SD	5.40	1.70	0.60	0.02	0.18	0.59	1.95	0.27	0.11	4.94	2.50	0.3	66.8	20.1	2.1	1.4	81.6	0.0	9.4

Chemistry of dust and soil parent materials from the LBA area.

CaCO<sub>3</sub> (Table 2). The Tertiary Santa Cruz Formation, a highly weathered Paleozoic marble unit in the Andean Cordillera, and carbonate-rich lacustrine sediments along the shores of LBA, were identified as likely sources for the carbonates. These interpretations are consistent with those in other semi-arid regions, including the Silver Lake playa in southeastern California (Reheis et al., 1989) and Kyle Canyon, Nevada (Reheis et al., 1992).

Excluding the extreme values of 27.1 and 21.4 g m<sup>-2</sup> yr<sup>-1</sup>, our data suggest an average deposition rate of 0.18 g m<sup>-2</sup> yr<sup>-1</sup> of CaCO<sub>3</sub> in dust (Table 2). Long-term accumulation rates (LTA) of CaCO<sub>3</sub> in soils of the LBA area are 0.32, 0.14, 0.14, and 0.042 g m<sup>-2</sup> yr<sup>-1</sup> on Fenix, Moreno, Deseado, and Telken drifts, respectively. The mean LTA value of 0.16 is comparable to the measured short-term dust deposition rate of 0.18 g m<sup>-2</sup> yr<sup>-1</sup> of CaCO<sub>3</sub>.

We compared the total elemental composition of dust that is from the surface A horizon of soils from the LBA

area. Compared with the topsoil, dust was enriched in Si, Al, K, and Sr and depleted in P and Na (Table 3). Our data are comparable to values reported for dust and topsoils in Patagonia by Gaiero et al. (2003). These data suggest that the dust originates from wind-eroded topsoil that is enriched in organic C (Table 2) and the weathered sediments mentioned previously that are enriched in CaCO<sub>3</sub>.

Péwé (1959) differentiated between sand- and ice-wedge casts. Sand-wedge casts tend to be thin, vertically foliated, and devoid of coarse fragments (Fig. 6B); in contrast, ice-wedge casts are broader, lack vertical foliation, and contain coarse fragments (Fig. 6D). Both are common in Moreno, Deseado, and Telken drifts. These cryogenic features appear to result from a periglacial climate, primarily during the last glacial maximum (LGM). In some cases cryogenesis has disrupted the calcrete layer (Fig. 6A). Fossil sand wedges generally are found only in dry climates such as Antarctica with continuous



Fig. 6. Effect of relict cryogenesis in selected soils of southern Patagonia: (A) a fossil sand or ice wedge on Telken IV drift showing infilling of the petrocalcic horizon with A horizon material; (B) a fossil sand wedge in outwash of mid-Pleistocene age near Río Gallegos showing the classical narrow form and vertically foliated structure; (C) cryoturbation in Sierra de los Frailes drift of mid-Pleistocene age near Río Gallegos; and (D) ice-wedge casts in multiple drifts near Río Gallegos.

permafrost and mean annual air temperature colder than  $-8\text{ }^{\circ}\text{C}$  (Péwé, 1959).

The existence of fossil sand wedges in southern Patagonia implies that the climate during the LGM may have been drier than the current  $100\text{--}200\text{ mm yr}^{-1}$  of precipitation and colder by as much as  $16\text{ }^{\circ}\text{C}$ . Trombotto (2002) proposed a similar change in temperature from fossil ice wedges in North Patagonia. However, other studies suggest that the mean annual air temperature was  $\sim 6\text{ }^{\circ}\text{C}$  cooler than modern at the height of the LGM in the Southern Hemisphere and perhaps a little drier at the LBA latitude, including glacier models (Hulton et al., 2002), fossil pollen records (Moreno et al., 2001) and ocean-core geochemistry (Lamy et al., 2004). Cryogenic features have reported throughout Patagonia, the Falkland Islands, and the Antarctic Peninsula (Vogt and del Valle, 1994; Trombotto, 1996, 2002).

The results of this study have important implications regarding the origin and timing of dust incorporated in Antarctic ice cores. Diekmann et al. (2000) suggested that the spikes in dust at Vostok and Dome C originated from the Patagonian outwash plains during glacial stages 2, 4, and 6. Stages 2 and 6 correspond to Fenix and Moreno drifts, but no terrestrial record of stage 4 has been identified at LBA. Vogt and del Valle (1994) suggest that much of the calcareous dust in Patagonia was deposited during glacial cycles when sea level was lowered by  $100\text{--}120\text{ m}$  and the continental shelf was widened by  $400\text{ to }1000\text{ km}$ . Our dust trap measurements suggest that carbonate deposition continues in the modern environment.

## 6. Conclusions

Carbonates in soils of LBA originate from dust rather than from pedogenic weathering in that (1) the till parent materials contain low amounts of  $\text{CaCO}_3$ , (2) there is minimal evidence for weathering of Ca-bearing minerals in the soil, (3) the amount of  $\text{CaCO}_3$  in the profile is far in excess of what could be released by weathering, (4) dust collected from the study area is enriched in  $\text{CaCO}_3$  ( $\sim 4\%$ ), and (5) a source area for the carbonates was identified northwest of the study near Lago General Carraras.

Our data suggest a current deposition rate of  $0.18\text{ g m}^{-2}\text{ yr}^{-1}$  of  $\text{CaCO}_3$ . The mean LTA calculated from soil profiles is  $0.16\text{ g m}^{-2}\text{ yr}^{-1}$  of  $\text{CaCO}_3$ . Therefore, the profile quantities of  $\text{CaCO}_3$  can be explained by contribution of carbonates in aeolian dust.

Pedogenic carbonates are important as a relative-age indicator in that the following properties increase with age of exposure: (1) thickness of the Bk+Bck horizons, (2) maximum carbonate stage, (3) profile accumulation of

pedogenic carbonates, and (4) mass flux of Ca from a geochemical mass balance.

Finally, pedogenic carbonates offer a promise for dating of sediments in Patagonia. Stage I carbonate pendants on a coarse-gravel clast from Deseado outwash were dated at  $224\text{ ky}$  from  $^{230}\text{Th}\text{--U}$  and thermal ionization mass spectrometry, which is consistent with dates obtained from cosmogenic dating.

## Acknowledgments

This project was supported by the National Science Foundation Earth System History grant ATM-0212450. We appreciate the assistance of A. Frank, M. Kaplan, S. McGee, D. Mickelson, J. Rabassa, and B. Singer. We are grateful for the logistic support and friendship of Reynaldo (Coco) and Joan (Petti) Nauta of Estancia Telken and the cooperation of all of the landowners in the Perito Moreno area. Dr. Warren Sharp kindly provided the  $^{230}\text{Th}\text{--U}$  ages for a clast on the Deseado outwash.

## References

- Basile, I., Grousset, F.E., Revel, M., Petit, J.R., Biscaye, P.E., Barkov, N.I., 1997. Patagonian origin of glacial dust deposited in East Antarctica (Vostok and Dome C) during glacial stages 2, 4 and 6. *Earth Planet. Sci. Lett.* 146, 573–589.
- Birkeland, P.W., 1999. *Soils and Geomorphology*, 3rd ed. Oxford Univ. Press, NY.
- Bockheim, J.G., Birkeland, P.W., Bland, W.L., 2000. Carbon storage and accumulation rates in alpine soils: evidence from Holocene chronosequences. *Advances in Soil Science: Global Climate Change and Cold Ecosystems*, Chap. 13. CRC Press, Boca Raton, FL, pp. 185–196.
- Brimhall, G.H., Dietrich, W.E., 1987. Constitutive mass balance relations between chemical composition, volume, density, porosity, and strain in metasomatic hydrochemical systems: results on weathering and pedogenesis. *Geochim. Cosmochim. Acta* 51, 567–587.
- Clapperton, C.M., 1993. *Quaternary Geology and Geomorphology of South America*. Elsevier, Amsterdam, New York. 779 p.
- Delmonte, B., Basile-Doelsch, I., Petit, J.-R., Maggi, V., Revel-Rolland, M., Michrad, A., Jagoutz, E., Grousset, F., 2004a. Comparing the Epica and Vostok dust records during the last 220,000 years: stratigraphical correlation and provenance in glacial periods. *Earth-Sci. Rev.* 66, 63–87.
- Delmonte, B., Petit, J.-R., Andersen, K.K., Basile-Doelsch, I., Maggi, V., Lipenkov, V.Y., 2004b. Dust size evidence for opposite regional atmospheric circulation changes over East Antarctica during the last climatic transition. *Clim. Dyn.* 23, 427–438.
- Diekmann, B., Kuhn, G., Rachold, V., Abelmann, A., Brathauer, U., Fütterer, D.K., Gersonde, R., Grobe, H., 2000. Terrigenous sediment supply in the Scotia Sea (Southern Ocean): response to Late Quaternary ice dynamics in Patagonia and on the Antarctic Peninsula. *Palaeogeogr. Palaeoclimatol. Palaeoecol.* 162, 357–387.

- Douglass, D.C., 2005. Glacial Chronology, Soil development, and paleoclimate reconstructions for mid-latitude South America, 1 Ma to Recent. PhD Dissertation, University of Wisconsin–Madison. 212 p.
- Douglass, D.C., Bockheim, J.G., 2006. Soil-forming rates and processes on Quaternary moraines near Lago Buenos Aires, Argentina. *Quat. Res.* 65, 293–307.
- FitzPatrick, E.A., 1993. *Soil Microscopy and Micromorphology*. J. Wiley & Sons, NY.
- Gaiero, D.M., Probst, J.-L., Depetris, P.J., Bidart, S.M., Leleyter, L., 2003. Iron and other transition metals in Patagonian riverborne and airborne materials: geochemical control and transport to the southern Atlantic Ocean. *Geochim. Cosmochim. Acta* 67, 3603–3623.
- Gile, L.H., Peterson, F.F., Grossman, R.B., 1966. Morphological and genetic sequences of carbonate accumulation in desert soils. *Soil Sci.* 101, 347–360.
- Hulton, N.R.J., Purves, R.S., McCulloch, R.D., Sugden, D.E., Bentley, M.J., 2002. The last glacial maximum and deglaciation in southern South America. *Quat. Sci. Rev.* 21, 233–241.
- INTA, 1995. *Atlas de suelos de la República Argentina*. Instituto de Suelos, INTA, Castelar.
- Kaplan, M.R., Ackert Jr., R.P., Singer, B.S., Douglass, D.C., Kurz, M.D., 2004. Cosmogenic nuclide chronology of millennial-scale glacial advances during O isotope stage 2 in Patagonia. *Geol. Soc. Amer. Bull.* 116, 308–321.
- Lamy, F., Kaiser, J., Ninnemann, U., Hebbeln, D., Arz, H.W., Stoner, J., 2004. Antarctic timing of surface water changes off Chile and Patagonian ice sheet response. *Science* 304, 1959–1962.
- MINITAB, Inc., 2000. Minitab statistical software. Release 13 for Windows.
- Monger, H.C., Daugherty, L.A., Gile, L.H., 1991. A microscopic examination of pedogenic calcite in an Aridisol of southern New Mexico. In: Nettleton, W.D. (Ed.), *Occurrence, characteristics, and genesis of carbonate, gypsum, and silica accumulation in soils*. SSSA Spec. Publ., vol. 26. Soil Sci. Soc. Am, Madison, WI, pp. 37–60.
- Moreno, P.I., Jacobson, G.L., Lowell, T.V., Denton, G.H., 2001. Interhemispheric climate links revealed by a late-glacial cooling episode in southern Chile. *Nature* 409, 804–808.
- National Center for Atmospheric Research, 2003. World Monthly Surface Station Climatology Dataset. National Center for Atmospheric Research. <http://dss.ucar.edu/datasets/ds570.0/>.
- Péwé, T.L., 1959. Sand-wedge polygons (tessellations) in the McMurdo Sound region, Antarctica — a progress report. *Am. J. Sci.* 257, 545–552.
- Rabenhorst, M.C., Wilding, L.D., 1986. Pedogenesis of the Edwards Plateau, Texas. III. New model for formation of petrocalcic horizons. *Soil Sci. Soc. Am. J.* 50, 693–699.
- Reheis, M.C., Harden, J.W., McFadden, L.D., Shroba, R.R., 1989. Development rates of late Quaternary soils, Silver Lake playa, California. *Soil Sci. Soc. Am. J.* 53, 1127–1140.
- Reheis, M.C., Sowers, J.M., Taylor, E.M., McFadden, L.D., Harden, J.W., 1992. Morphology and genesis of carbonate soils on the Kyle Canyon fan, Nevada, U.S.A. *Geoderma* 52, 303–342.
- Schlesinger, W.H., 1990. Evidence from chronosequence studies for a low carbon-storage potential of soils. *Nature* 348, 232–234.
- Schoeneberger, P.J., Wysocki, D.A., Benham, E.C., Broderson, W.D., 2002. *Field Book for Describing and Sampling Soils*. National Soil Survey Center, Natural Resources Conservation Service, U.S. Department of Agriculture, Lincoln, NE.
- Sharp, W.D., Ludwig, K.R., Chadwick, O.A., Amundson, R., Glaser, L.L., 2003. Dating fluvial terraces by  $^{230}\text{Th}/\text{U}$  on pedogenic carbonate, Wind River basin, Wyoming. *Quat. Res.* 59, 139–150.
- Singer, B.S., Ackert Jr., R.P., Guillaou, H., 2004.  $^{40}\text{Ar}/^{39}\text{Ar}$  and K–Ar chronology of Pleistocene glaciations in Patagonia. *Geol. Soc. Amer. Bull.* 116, 434–450.
- Smith, J., Vance, D., Kemp, R.A., Archer, C., Toms, P., King, M., Zárate, M., 2003. Isotopic constraints on the source of Argentinian loess—with implications for atmospheric circulation and the provenance of Antarctic dust during recent glacial maxima. *Earth Planet. Sci. Lett.* 212, 181–196.
- Soil Survey Staff, 1996. *Soil Survey Laboratory Methods Manual*. Soil Survey Investigations Report No. 42, V. 3.0. National Soil Survey Center, Natural Resources Conservation Service, U.S. Department of Agriculture, Lincoln, NE.
- Soriano, A., 1983. Deserts and semi-deserts of Patagonia. In: West, N.E. (Ed.), *Temperate Deserts and Semi-deserts. Ecosystems of the World*, vol. 5. Elsevier, Amsterdam, pp. 423–460.
- Trombotto, D., 1996. The old cryogenic structures of northern Patagonia: the Cryomere Perford. *Z. Geomorphol.* 40 (3), 385–399.
- Trombotto, D., 2002. Inventory of fossil cryogenic forms and structures in Patagonia and the mountains of Argentina beyond the Andes. *S. Afr. J. Sci.* 98, 171–180.
- Vogt, T., del Valle, H.F., 1994. Calcretes and cryogenic structures in the area of Puerto Madryn (Chubut, Patagonia, Argentina). *Geogr. Ann., Ser. A.* 7, 57–75.
- Zárate, M.A., 2003. Loess of southern South America. *Quat. Sci. Rev.* 22, 1987–2006.